JOURNAL OF SPACECRAFT AND ROCKETS
Vol. 44, No. 3, May–June 2007

Experimental and Numerical Correlation of Gravity Sag in Solar-Sail-Quality Membranes

Jonathan T. Black*
University of Kentucky, Lexington, Kentucky 40506
Jack Leifer†
Trinity University, San Antonio, Texas 78212
Joshua A. DeMoss‡
Virginia Polytechnic Institute and State University, Blacksburg, Virginia 24061
and
Eric N. Walker§
George Washington University and NASA Langley Research Center, Hampton, Virginia 23681

DOI: 10.2514/1.20958

Solar sails are among the most studied members of the ultralightweight and inflatable (gossamer) space structures family, due to their potential to provide propellantless propulsion. They are comprised of ultrathin membrane panels that, to date, have proven very difficult to experimentally characterize and numerically model, due to their reflectivity and flexibility and the effects of gravity sag and air damping. Numerical models must be correlated with experimental measurements of subscale solar sails as the first step in verifying that the models can be scaled up to represent full-sized solar sails. In this paper, the surface shapes of two horizontally-supported 25-μm-thick aluminized Kapton membranes were measured to a 1.0-mm resolution using photogrammetry. Simple numerical models were developed and their output matched the corresponding experimental data in all cases with less than 33% error. This correlation between the numerical predictions and the experimental data is in line with similar results obtained by others who used more complex numerical models to predict the gravity-induced sag of larger sail panels. The results indicate that the largest source of discrepancy between predicted and measured data is membrane slack. It is postulated that incorporation of geometric slack into the numerical models would likely reduce this discrepancy.

I. Introduction

SUCCESSFUL deployment and on-mission control of membrane-based gossamer structures can only occur through the design and use of validated full-scale numerical models. Although subscale numerical models can be verified through precision experimental measurement of corresponding subscale physical structures, it would be impossible to accomplish such direct verification of full-scale structures on Earth. This verification is impossible because full-scale physical models of square solar sails or other large membrane space structures are envisioned to exceed 100 m or more on a side, far exceeding the capacity of available vacuum chambers and current procedures that compensate for the effects of gravity. Because direct validation of the desired full-scale high-fidelity numerical models cannot be achieved using current technology, they must instead be verified indirectly, by first correlating subscale numerical models with measurements using subscale physical test structures, altered to eliminate the influences of gravity and air damping, and then scaled up to reflect the full size of the deployed structure.

As an initial step in the subscale model correlation and verification process, several solar-sail-quality membranes were suspended horizontally from an aluminum frame. The static shape of each membrane under gravity load was measured using a full-field, noncontact technique called *dot-projection photogrammetry*. Other commonly used measurement methods such as scanned laser Doppler vibrometry are not truly full-field measurements because data are obtained sequentially at each specified measurement point. Alternative approaches, including strain gauges, are single-point measurement methods that tend to introduce extraneous loads to the point at which they are attached to the membrane. The data obtained via the dot-projection photogrammetry measurements discussed herein are compared with results from numerical models that contain ideal approximations of the physical boundary and suspension conditions present in the subscale test articles.

The work contained herein parallels similar recent efforts put forth to predict gravity deflection of solar sail membranes. These include that of Sleight et al. [1], who predicted the sagged shape of a 20-m, 4-quadrant solar sail system using an ABAQUS model consisting of over 45,000 membrane elements and over 25,000 nodes. The study found that "the ABAQUS analysis. . .underpredicted the sail billow by about 25% compared with the photogrammetry test data [1]." Johnston et al. [2] predicted the gravity-induced sag of a single triangular quadrant of a 2-m scale model of a 4-quadrant corner-attached solar sail. The test setup enabled measurement of the sag under various tension loads and inclinations to vertical. For the horizontally oriented case, the ABAQUS model consisting of 11,645 shell elements and 11,895 nodes underpredicted the experimental

Presented as Paper 1579 at the 45th AIAA/ASME/ASCE/AHS/ASC Structures, Structural Dynamics & Materials Conference, Palm Springs, CA, 19–22 April 2004; received 7 November 2005; revision received 27 November 2006; accepted for publication 27 November 2006.

*Graduate Research Assistant, Department of Mechanical Engineering; currently Assistant Professor, Department of Aeronautics and Astronautics, U.S. Air Force Institute of Technology, Wright–Patterson Air Force Base, OH 45433. Member AIAA.

†Assistant Professor, Department of Engineering Science. Member AIAA.

‡Co-Op Student, Department of Aerospace Engineering. Student Member AIAA.

§Graduate Research Assistant, Structural Dynamics Branch. Student Member AIAA.

measurements by an average of 24% for all preloads. Taleghani et al. [3] predicted the deflected shape of a 10-m, 4-quadrant solar sail system including support members. The MSC-NASTRAN model consisting of 5435 structural elements and 2856 nodes exhibited discrepancies, with experimental values ranging from 0.4 to 13.4%.

The goals of this study include demonstrating that small, simple shell element models in ANSYS are capable of achieving results similar to the much larger and more detailed models discussed earlier, as well as showing that simple approximations of boundary conditions are as effective as the more complex approach used by the more detailed numerical models. Descriptions of the numerical models and subscale structures used are presented in the following sections. The experimental measurements and numerical results are then presented and discussed within the context of the previously reported work.

II. Background

Solar sails, sun shades, and membrane apertures are part of the class of ultralightweight and inflatable gossamer space structures. Specifically, solar sails are propellantless propulsion devices that generate a small but continuous acceleration on the order of $1.00\ \mathrm{mm/s^2}$. To achieve this threshold acceleration, solar sails must be fabricated using membranes less than 5.0-μm thick, with areal densities less than $7.0\ \mathrm{g/m^2}$ [4]. The thrust provided by a solar sail is generated when photons of sunlight are reflected by their specular surfaces, causing the momentum transfer that propels the spacecraft. This momentum transfer, called solar pressure, is quite small [$9.12 \times 10^{-6}\ \mathrm{N/m^2}$ at 1 AU (astronomical unit)] and requires that the sails be both very large and very lightweight to reach a useful acceleration level under such conditions. The continuous availability of propulsion force provided by momentum transfer between photons and the surface of the solar sail has been predicted to enable the achievement of non-Keplerian orbits [5]. Furthermore, solar-sail-based spacecraft have the potential to shorten the duration of missions (over those using conventional spacecraft that rely on gravity assists) such as payload delivery to inner solar orbits of less than 0.5 AU and sample return missions [5]. Consequently, solar sails (such as the illustration shown in Fig. 1) have been proposed for use on several NASA missions [6,7]. In addition to their potential use as a means of propulsion, this type of thin gossamer membrane has been proposed for use in other space applications, including telescope sun shades and inflatable apertures [8].

III. Test Articles and Experimental Setup

Two aluminum frames, one of which is shown in Fig. 2, were bolted to a steel backstop in a horizontal orientation approximately 2.8 m above the ground. Each frame used was designed to accommodate one particular membrane geometry. The horizontal orientation, in which the gravity vector is directed approximately normal to the sail surface, was chosen to reflect the loading geometry of actual solar sails. Although solar pressure is six orders of magnitude smaller than the force of gravity, it will be incident roughly normal to the surface of the sail [5]. The backstop-bolting scheme used parallel horizontal tracks that maintained the adjacent frame edge in the desired horizontal configuration. The protruding corners of the frame were supported by steel tension wires that were also connected to the backstop. This extra cantilevered support was provided to eliminate as much bending of the aluminum frame as possible. Two separate 25-μm-thick aluminized Kapton membranes were measured, one was square in shape, 1.0 m per side, and one was right-triangle-shaped with two 1.0-m legs. Each membrane was attached to the frame at the corners (corner-supported) by hand using adhesive with the intention of creating a condition in which no prestress or slack was present. The area behind (above) the membranes was open, allowing them to sag and wrinkle freely.

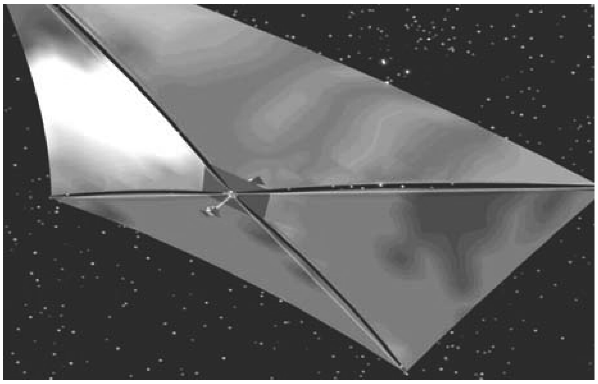
Fig. 1 Solar sail concept.

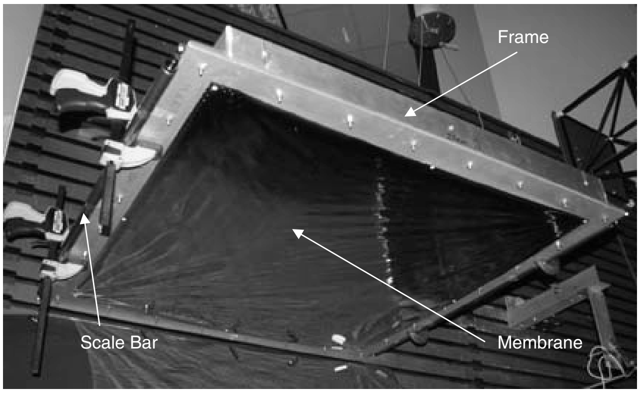

Fig. 2 Horizontally suspended aluminum frame with a corner-supported square membrane.

Dot-projection photogrammetry was used to statically characterize the out-of-plane surface shape of each suspended membrane that was tested. Photogrammetry is the science of making precise shape measurements from photographs. Generically, a grid of circular high-contrast retroreflective targets is attached to the object to be characterized. Multiple underexposed images, each from a different angle, are captured using a flash to yield binary images of white targets on a black background. The images are loaded into commercially available software (PhotoModeler 5.2) that enables the centroid of each target imaged in the membrane to be precisely located in three dimensions. The software facilitates the image analysis as follows: each image is loaded into the software and then associated with the camera-calibration parameters that allow the removal of distortions in the images caused by lens curvature and imperfections, focus, aperture setting, and other camera factors and aberrations. The centers of the white targets are marked to subpixel accuracy using an automatic least-squares-matching algorithm, and marks corresponding to the same target on each image are associated with each other. The three-dimensional camera and target locations are then triangulated iteratively. The final product is a set of three-dimensional point locations that is exported for analysis and visualization. A much more detailed description of the process is presented in [9–12].

The projector setup shown in Fig. 3 was used to create a grid of targets on each membrane instead of physically attaching targets, which would have added significant mass to the membranes and altered their responses. Four Kodak 760M 6.0-megapixel monochrome digital cameras imaged these fields of approximately 3200 and approximately 1800 targets for the square and triangular membranes, respectively. The photographs were taken simultaneously to minimize the possibility of membrane movement between images caused by either temperature changes or stray air currents in the laboratory space. An example of an actual image used in the data processing is shown in Fig. 4.

All photogrammetry measurements are initially unscaled, meaning that a scale and orientation were defined in postprocessing. Invar scale bars (Figs. 2 and 3) with targets exactly 1.1176 m (44.000 in.) apart were used to scale the project. Because the retroreflective targets on the scale bar required a flash for

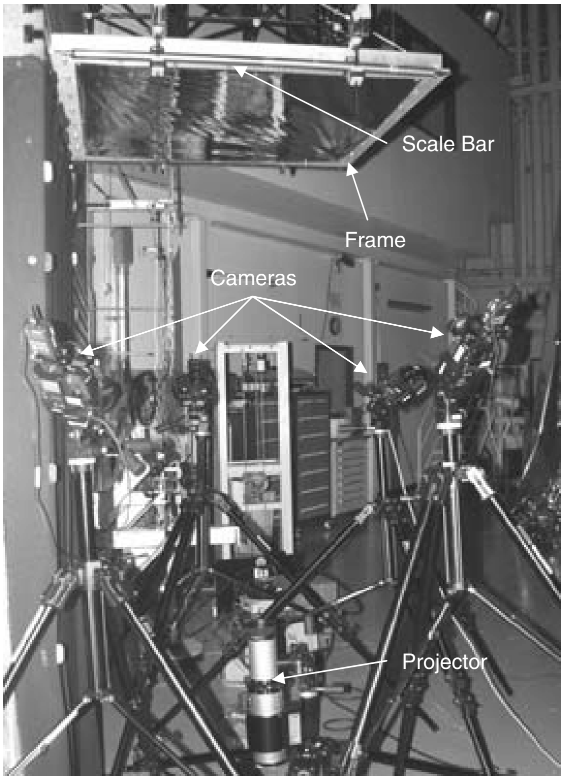

Fig. 3 Test setup.

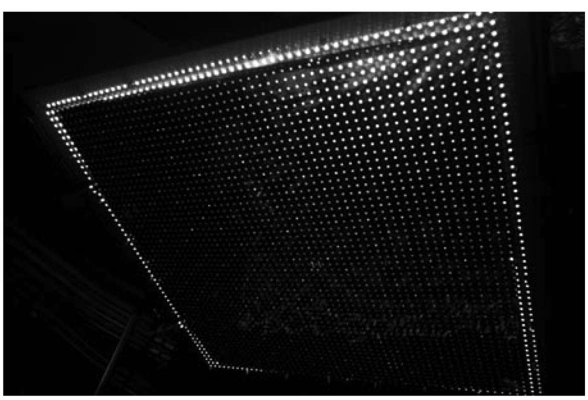

Fig. 4 Image used in data processing.

illumination, three additional images were taken after the measurement images were captured and referenced back to the four simultaneous images using projected and attached targets on the frame.

IV. Experimental Results

The surface profile obtained for the first suspended test article, the square Kapton membrane, is shown in Fig. 5. This profile was generated from the grid of 3200 three-dimensional target locations exported from the photogrammetry software. A large, nearly symmetric sag of approximately 19 mm in amplitude is visible, as well as some smaller wrinkles that extend from the corners to the center of the membrane. The accuracy of this measurement was determined by comparing the distance between the targets of the second scale bar (shown in Fig. 3), measured with photogrammetry, with the actual distance and was calculated to be ±0.5 mm.

Using the same approach, the surface shape of the right-triangle-shaped membrane attached to the frame at its corners was generated and is shown in Fig. 6. A large, nearly symmetric sag in the membrane approximately 15 mm in depth at its maximum point was

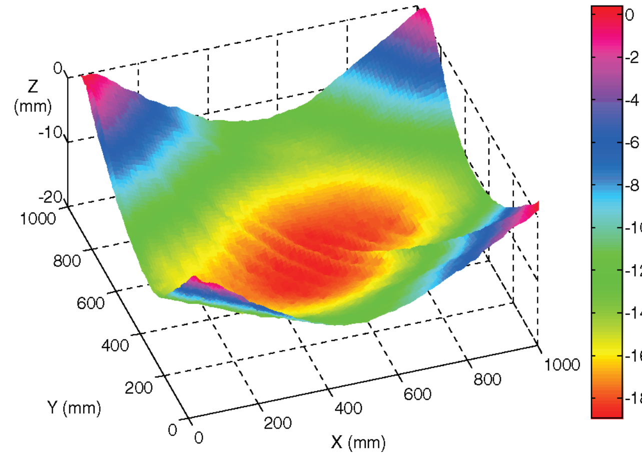

Fig. 5 Measured sag (mm) of corner-attached square membrane.

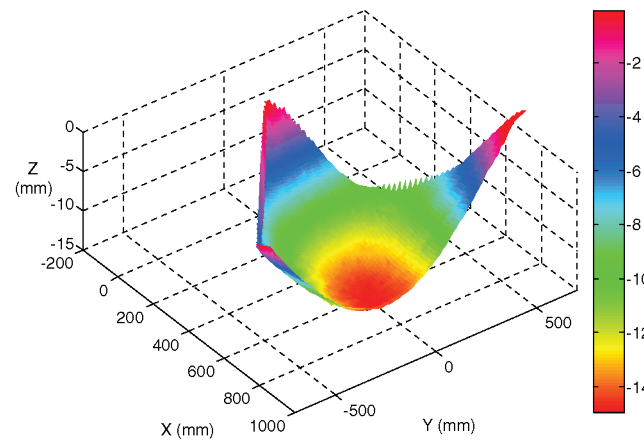

Fig. 6 Measured sag (mm) of a corner-attached triangular membrane.

observed, and no wrinkling is visible. The accuracy of the measurement for this specimen was also calculated to be ±0.5 mm.

V. Finite Element Models and Results

Finite element models were created in ANSYS corresponding to the membrane geometries (square and right-triangle) that were tested using photogrammetry. To reflect the loading geometry imparted by the solar pressure (normal to the initial orientation of the surface), each membrane was aligned horizontally, perpendicular to the gravity vector that was oriented downward through the sail surface within the model. The finite element models created for each specimen used SHELL181 elements with four nodes and six degrees of freedom per node. SHELL181 elements were chosen in lieu of SHELL63 elements because they are specifically well suited for large-displacement nonlinear analyses [13]. To reflect the idealized geometry of the physical models, 0.002-m, 45-deg chamfers were created at each corner of the finite element models, and nodal degrees of freedom located along each chamfer were fixed. For the square membrane, x- and y-axis symmetry was assumed, and so only one-quarter of the membrane surface was simulated using a total of 2561 elements and 2661 nodes. For the triangular membrane, symmetry along the diagonal was assumed, and one-half of the membrane surface was simulated using a total of 1135

Table 1 Material properties for Kapton type 100 Hn film [13–15]

Property	Value
Young's modulus E	2.5 GPa
Poisson's ratio υ	0.34
Density ρ	1420 kg/m^2

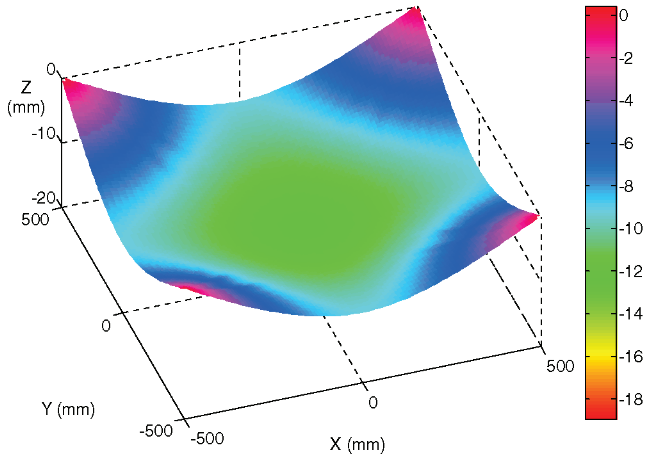

Fig. 7 Predicted out-of-plane sag (mm) of a corner-supported square membrane.

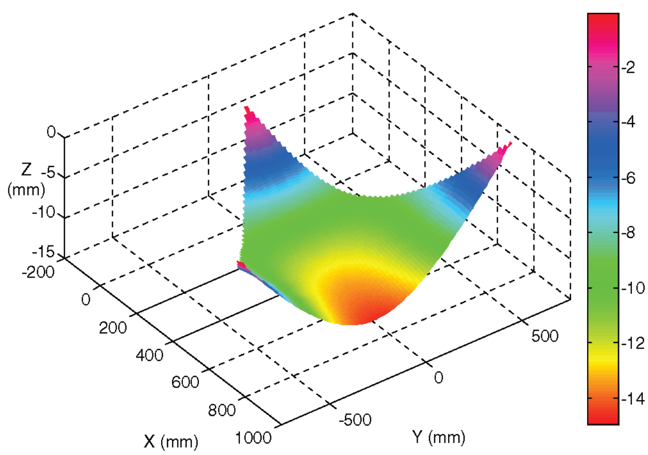

Fig. 8 Predicted out-of-plane sag (mm) of a corner-supported triangular membrane.

elements and 1215 nodes. The material properties for Kapton type 100 Hn film that were associated with each shell element are shown in Table 1.

The predicted sags of the square and triangular membranes considered herein are presented in Figs. 7 and 8 on the same scales as with the experimental data in Figs. 5 and 6 to allow comparison.

The static, large deformation nonlinear analysis that resulted in the gravity-induced sags apparent in Figs. 7 and 8 were obtained using the arc-length method [11]. The arc-length method applied gravity in 239 substeps, iteratively varying the applied load at each equilibrium convergence calculation within each substep to maintain total model convergence. The models were designed with simplicity in mind, and the element sizes of 0.010 and 0.015 m^2, respectively, for the square and triangular geometries, were expected to provide sufficient fidelity to show the overall gravity-induced sagging behavior of each membrane. Despite the intentional simplicity of the models, a minimum of 5 h of computer processor time was required to generate each of the results.

VI. Correlation

An examination of Figs. 5 and 7 and the side-by-side contour plots in Fig. 9 enables a comparison of the experimental results and the finite element simulation for the square membrane. The numerical results in Figs. 7 and 9 show a gravity sag of 12.5 mm, whereas the experimental data show a sag of approximately 18.5 mm. The two data sets have similar diamond-shaped global-deflection patterns and similar small-amplitude wrinkles running from the corners to the centers of the membranes. Figure 9 also clearly shows some asymmetry in the experimental results. A comparison between the experimental and simulated sags obtained for the triangular membrane (Figs. 6 and 8, respectively) and the side-by-side contour plots in Fig. 10 also show similarities. The figures reveal a maximum gravity-induced deflection of 15.0 mm, as well as a similar overall shape. No wrinkle pattern is visible in either the experimental or numerical data, and the experimental data again show asymmetry.

The two-dimensional (2-D) cuts through the experimental and finite element data of the square membrane shown in Fig. 11 help to explain why the finite element simulation underpredicted the experimental data. If the membrane had been perfectly attached to the frame as idealized in the finite element boundary conditions, all of the 2-D cuts of the experimental data would have a minimum in the exact center of the curve and lie directly on top of one another, as do the perfectly symmetric finite element results. Figure 11, however, shows that the minima of the experimental data cuts are slightly offset to either side of center, indicating that the membrane was most likely not attached to the frame symmetrically (also noted in Fig. 9). Possible additional sources of asymmetry include variations in membrane thickness, application of different quantities of adhesive at each attachment location, asymmetrical membrane shape, nonlevel frame, etc. The result of the lack of symmetry in the attachment was a small amount of initial slack in the membrane that was not modeled in the finite element simulation. A few millimeters of slack or asymmetry at the corner attachment locations of a 1-m^2 membrane would have been virtually unavoidable in the process of attaching it with adhesive by hand to the frame. This slack could easily be responsible, along with the unpredictable contraction of the adhesive during cure, for several millimeters of $-z$ deflection, in addition to that caused by gravity.

The asymmetry seen in the experimental data of the triangular membrane in Fig. 10 also resulted in some underprediction by the finite element simulation. If the membrane had been perfectly attached to the frame, the 2-D cut through the membrane center in Fig. 12 would have revealed a perfectly smooth curve with its minimum at the free edge, matching the finite element data. The center cut in Fig. 12, however, reveals that the experimentally measured maximum deflection (curve minimum) actually occurred just before the edge of the membrane, and it curled up slightly at the free edge along the hypotenuse of the membrane, creating a lip. As in

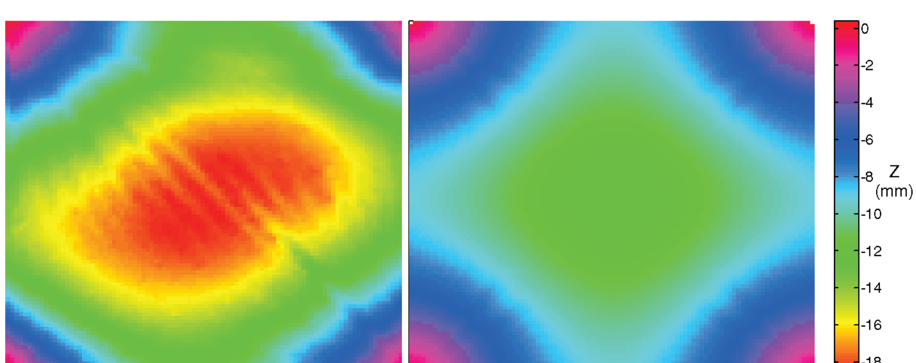

Fig. 9 Contour plots of measured (left) and predicted (right) out-of-plane sag (mm) of a corner-supported square membrane.

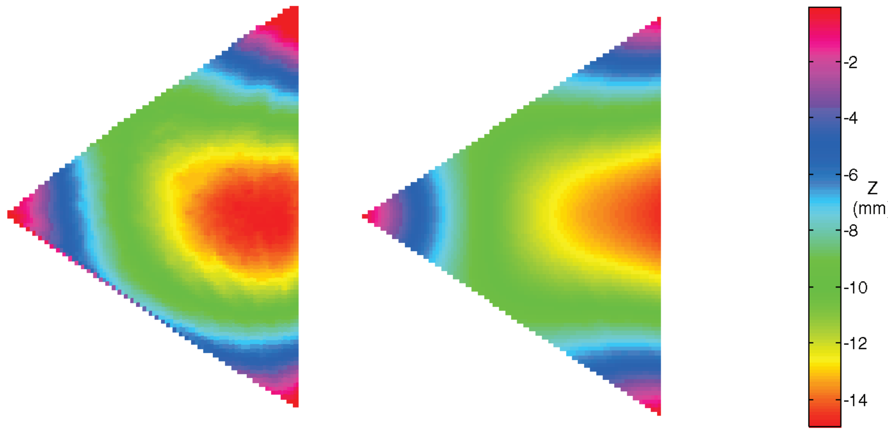

Fig. 10 Contour plots of measured (left) and predicted (right) out-of-plane sag (mm) of a corner-supported triangular membrane.

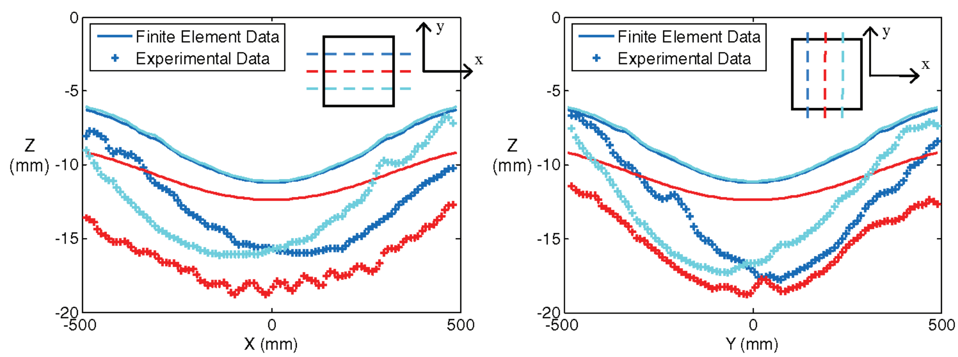

Fig. 11 Two-dimensional cuts through the membrane of measured and predicted out-of-plane sag (mm) of a corner-supported square membrane.

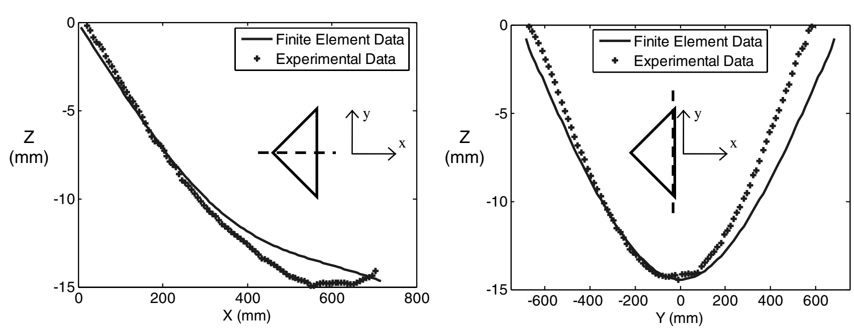

Fig. 12 Two-dimensional cuts through the membrane of measured and predicted out-of-plane sag (mm) of a corner-supported triangular membrane.

the preceding square membrane data, this asymmetry was caused by inherent inaccuracies in the hand-attachment process using adhesive and resulted in several millimeters of slack that were not modeled in the finite element simulation and led to the error.

To assess the quality of the experimental/numerical correlation, the results obtained herein were compared with those reported by others who conducted correlation studies on larger sail models, all performed subsequent to this one [1–3]. Each of the cited works used photogrammetry to measure gravity-induced sag and compared the experimental results with predictions provided by their own very large and detailed numerical simulations that extensively modeled the attachment of the membrane to its support structure. A summary of the pertinent results is provided in the Introduction.

The experimental versus numerical correlation obtained in this study is in line with the similar correlations obtained by others pursuing similar work. The variety of software packages and element types used for the simulations, as well as the range of sail dimensions studied (1–20 m) leads to the observation that neither scale nor model complexity seems to affect the numerical/experimental correlation. This could imply that numerical models will scale to full size (simulating sails for which the sides are an order of magnitude larger than those studied in any of the work cited herein) without affecting correlation. However, verification of such model insensitivity to scale and complexity can only be achieved by correlating measurement results obtained using a scaled sequence of physical test articles to predictions obtained using a single numerical-modeling approach (e.g., same FE software, fixed mesh density, or boundary conditions) over the range of scales evaluated. It should also be noted that none of the previous work studied the effect of incorporating slack into the models.

VII. Conclusions

The correlation of numerical models with experimental data is an important step in the future development of solar sails and other gossamer membrane structures. As an initial step in the process, small square and triangular solar-sail-quality membranes were suspended horizontally and supported at their corners. These simple support configurations enabled the use of relatively simple numerical models. Results obtained using the numerical models correlated to within 33% of the experimental data. Viewed alongside results achieved by similar projects that evaluated larger membranes and more complex numerical models, the correlation precision achieved here was quite comparable. Comparison of experimental and numerical data also strongly suggests that the most significant source of error was initial slack in the membrane, resulting from minor asymmetry in the suspension of the membrane, and that the addition of slack to the models or its removal from the experimental setup would greatly improve model accuracy. The methods and techniques used to create and validate the models are intended to demonstrate the potential of these experimental and numerical techniques for use in the creation of indirectly verified numerical models that will aid in the deployment and control of full-scale gossamer structures.

Acknowledgments

Portions of this work were performed under a Graduate Research Scholar Assistantship provided by the NASA Langley Research Center through George Washington University and a NASA Graduate Student Research Program fellowship through the University of Kentucky, grant number NNL04AA21H, Richard Pappa, advisor. The authors would like to thank Richard Pappa, Jessica Woods-Vedeler, and Keith Belvin of the NASA Langley Research Center and Vaughn Behun of Swales Aerospace for their materials, hardware, and testing support.

References

[1] Sleight, D., Mann, T., Lichodziejewski, D., and Derbes, B., "Structural Analysis and Test Comparison of a 20-Meter Inflation-Deployed Solar Sail," 47th AIAA/ASME/ASCE/AHS/ASC Structures, Structural Dynamics, and Materials Conference, Newport, RI, AIAA Paper 2006-1706, May 2006.

[2] Johnston, J. D., Blandino, J. R., and McEvoy, K. C., "Analytical and Experimental Characterization of Gravity Induced Deformations in Subscale Gossamer Structures," *Journal of Spacecraft and Rockets*, Vol. 43, No. 4, July–Aug. 2006, pp. 762–770.

[3] Taleghani, B., Lively, P., Gaspar, J., Murphy, D., and Trautt, T., "Dynamic and Static Shape Test/Analysis Correlation of a 1- Meter Quadrant Solar Sail," 46th AIAA/ASME/ASCE/AHS/ASC Structures, Structural Dynamics, and Materials Conference, Austin, TX, AIAA Paper 2005-2123, Apr. 2005.

[4] Spieth, D., and Zubrin, R., "Ultra-Thin Solar Sails for Interstellar Travel: Phase 1 Final Report," *NASA Institute for Advanced Concepts*, Pioneer Astronautics Inc., Lakewood, CO, Dec. 1999.

[5] McInnes, C. R., *Solar Sailing: Technology, Dynamics and Mission Applications*, Praxis, Chichester, England, U.K., 1999.

[6] McInnes, C. R., "GEOSAIL: Exploring the Geomagnetic Tail Using a Small Solar Sail," *Journal of Spacecraft and Rockets*, Vol. 38, No. 4, July–Aug 2001, pp. 622–629.

[7] West, J. L., and Derbes, B., "Solar Sail Vehicle System Design for the GEOStorm Warning Mission," AIAA Paper 2000-5326, 2000.

[8] Johnston, J., and Parrish, K., "Thermal-Structural Analysis of Sunshield Membranes," AIAA Paper 2003-1904, Apr. 2003.

[9] Pappa, R. S., Jones, T. W., Black, J. T., Walford, A., Robson, S., and Shortis, M. R., "Photogrammetry Methodology Development for Gossamer Space Structures," *Sound and Vibration*, Vol. 36, No. 8, Aug. 2002, pp. 12–21.

[10] Pappa, R. S., Black, J. T., Blandino, J. R., Jones, T. W., Danehy, P. M., and Dorrington, A. A., "Dot Projection Photogrammetry and Videogrammetry of Gossamer Space Structures," *Journal of Spacecraft and Rockets*, Vol. 40, No. 6, Nov.–Dec. 2003, pp. 858–867.

[11] Mikhail, E. M., Bethel, J. S., and McGlone, J. C., *Introduction to Modern Photogrammetry*, Wiley, New York, 2001.

[12] Black, J., "Photogrammetry and Videogrammetry Methods Development for Solar Sail Structures," M.S. Thesis, Joint Inst. for Advancement of Flight Sciences, NASA Langley Research Center, George Washington Univ., Hampton, VA, Sept. 2003; also NASA CR-2003-212678.

[13] Leifer, J., and Belvin, W. K., "Prediction of Wrinkle Amplitudes in Thin Film Membranes Using Finite Element Modeling," AIAA Paper 2003-1983, Apr. 2003.

[14] ANSYS, Software Package, Ver. 6.1, ANSYS, Inc., Canonsburg, PA, 2002.

[15] Anon., "Summary of Properties for Kapton Polyimide Films," *Kapton Polyimide Film* [online database], http://www.dupont.com/kapton/ [retrieved 15 Nov. 2006].

M. Nemeth
Associate Editor